J Physiol 597.11 (2019) pp 2867–2885

The Journal of Physiology

Intercellular calcium waves integrate hormonal control of glucose output in the intact liver

Lawrence D. Gaspers*, Nicola Pierobon* and Andrew P. Thomas

Department of Pharmacology, Physiology and Neuroscience, New Jersey Medical School Rutgers, The State University of New Jersey, Newark, NJ, USA

Edited by: Kim Barrett & Pawel Ferdek

Key points

- Sympathetic outflow and circulating glucogenic hormones both regulate liver function by increasing cytosolic calcium, although how these calcium signals are integrated at the tissue level is currently unknown.
- We show that stimulation of hepatic nerve fibres or perfusing the liver with physiological concentrations of vasopressin only will evoke localized cytosolic calcium oscillations and modest increases in hepatic glucose production.
- The combination of these stimuli acted synergistically to convert localized and asynchronous calcium responses into co-ordinated intercellular calcium waves that spread throughout the liver lobule and elicited a synergistic increase in hepatic glucose production.
- The results obtained in the present study demonstrate that subthreshold levels of one hormone can create an excitable medium across the liver lobule, which allows global propagation of calcium signals in response to local sympathetic innervation and integration of metabolic regulation by multiple hormones. This enables the liver lobules to respond as functional units to produce full-strength metabolic output at physiological levels of hormone.

Abstract Glucogenic hormones, including catecholamines and vasopressin, induce frequency-modulated cytosolic Ca^{2+} oscillations in hepatocytes, and these propagate as intercellular Ca^{2+} waves via gap junctions in the intact liver. We investigated the role of co-ordinated Ca^{2+} waves as a mechanism for integrating multiple endocrine and neuroendocrine inputs to control hepatic glucose production in perfused rat liver. Sympathetic nerve stimulation elicited localized Ca^{2+} increases that were restricted to hepatocytes in the periportal zone. During

Lawrence Gaspers is an Associate Professor in the Department of Pharmacology, Physiology and Neuroscience at Rutgers, New Jersey Medical School. He has developed confocal microscopy techniques for measuring hormone-induced calcium increases in hepatocytes within the intact perfused liver as a postdoctoral fellow in Andrew Thomas's laboratory at Thomas Jefferson University. **Nicola Pierobon** trained in the laboratory of Marisa Brini at the University of Padova before joining Andrew Thomas's laboratory at Rutgers, New Jersey Medical School, where he obtained his PhD. He has developed experimental approaches integrating electrical stimulation with intact tissue calcium signalling and glucose output. **Andrew Thomas** is Professor and Chair of the Department of Pharmacology, Physiology and Neuroscience at Rutgers, New Jersey Medical School, and Senior Associate Dean of School of Graduate Studies. He has worked on the dynamics of calcium signalling and its role in the regulation of liver function and also has developed the concept of signal integration through the architecture of the hepatic lobule functioning as an excitable syncytium. His research team is interested in understanding the molecular mechanisms underlying the generation of inositol 1,4,5-trisphosphate-dependent calcium spikes and calcium waves, as well as how aberrant Ca^{2+} signals contribute to the onset and development of liver pathologies.

*These authors contributed equally to this work.

DOI: 10.1113/JP277650

perfusion with subthreshold vasopressin, sympathetic stimulation converted asynchronous Ca^{2+} signals in a limited number of hepatocytes into co-ordinated intercellular Ca^{2+} waves that propagated across entire lobules. A similar synergism was observed between physiological concentrations of glucagon and vasopressin, where glucagon also facilitated the recruitment of hepatocytes into a Ca^{2+} wave. Hepatic glucose production was significantly higher with intralobular Ca^{2+} waves. We propose that inositol 1,4,5-trisphosphate (IP_3)-dependent Ca^{2+} signalling gives rise to an excitable medium across the functional syncytium of the hepatic lobule, co-ordinating and amplifying the metabolic responses to multiple hormonal inputs.

(Received 18 January 2019; accepted after revision 8 April 2019; first published online 10 April 2019)
Corresponding author A. P. Thomas: Department of Pharmacology, Physiology and Neuroscience, New Jersey Medical School Rutgers, The State University of New Jersey, Newark, NJ 07103, USA. Email: andrew.thomas@rutgers.edu

Introduction

Liver function is regulated by systemic hormones and by neuronal inputs from the central nervous system. The efferent innervations consist of both the sympathetic and the parasympathetic system, which originate from three major areas of the hypothalamus: the ventromedial hypothalamus (VMH), the lateral hypothalamic area (LHA) and the paraventricular hypothalamic nucleus (Shimazu, 1987, 1996; Buijs *et al.* 2003). In the mid-1800s, French physiologist Claude Bernard published his studies on the role of liver in carbohydrate metabolism, the discovery of glycogen, and the connection between brain and liver metabolism. He showed that puncture of the fourth ventricle in the brain induced hyperglycaemia in rabbits (Bernard, 1854). More than 100 years later, investigators started to clarify details of the hypothalamic connections with liver and blood glucose regulation. Stimulation of the VMH induced a rapid increase in blood glucose level and correlated with a pronounced decrease of liver glycogen, whereas LHA stimulation produced a slight decrease in blood glucose without affecting liver glycogen content (Shimazu *et al.* 1966). Electrical stimulation of the postganglionic sympathetic fibres, derived from the splanchnic nerve, produced a similar effect to VMH stimulation, with an increase of glycogen phosphorylase and glucose 6-phosphatase activities in the liver (Shimazu & Fukuda, 1965). Thus, it became clear that the sympathetic areas of the hypothalamus could accelerate glycogenolysis and affect other metabolic aspects in liver.

Studies investigating the central control of liver metabolism and haemodynamics *in vivo* were supplemented with experiments using isolated perfused liver, which has the advantage of excluding systemic endocrine contributions. In this *ex vivo* preparation, electrical stimulation of the nerve bundles surrounding the portal vein and hepatic artery excites both sympathetic and parasympathetic nerves. However, the sympathetic response predominates and the parasympathetic effects can only be studied if the sympathetic action is inhibited pharmacologically (Gardemann & Jungermann, 1986). It was shown that the intrinsic sympathetic innervation directly regulates liver glucose output (Niijima & Fukuda, 1973; Hartmann *et al.* 1982; Gardemann *et al.* 1992). Along with the stimulation of glycogenolysis, sympathetic output has also been shown to increase gluconeogenesis at the same time as suppressing glycolysis (Shimazu & Ogasawara, 1975), as well as enhancing hepatic very low density lipoprotein-triglyceride production (Bruinstroop *et al.* 2012), inducing a shift from lactate uptake to output (Hartmann *et al.* 1982; Gardemann *et al.* 1987; Gardemann *et al.* 1992) and decreasing hepatic ketogenesis (Beuers *et al.* 1986; Yamamoto *et al.* 1995). These effects are mainly the result of α_1-adrenergic stimulation by the neurotransmitter norepinephrine because they are almost completely abolished by α-adrenergic antagonists such as phentolamine and prazosin (Hartmann *et al.* 1982; Ulken *et al.* 1991).

Glucogenic hormones, such as norepinephrine and vasopressin, activate phosphorylase and increase hepatic glucose output via increases in cytosolic free calcium levels ($[Ca^{2+}]_c$) (Assimacopoulos-Jeannet *et al.* 1977; Blackmore *et al.* 1978; Garrison *et al.* 1979; Thomas *et al.* 1984; Binet *et al.* 1985; Exton, 1987). This is achieved by the activation of receptor-coupled phosphoinositide-specific phospholipase C ß to produce the Ca^{2+}-mobilizing second messenger, inositol 1,4,5-trisphosphate (IP_3) (Berridge, 2016). In hepatocytes, physiological concentrations of hormone evoke periodic baseline-separated Ca^{2+} spikes, or oscillations, that propagate throughout the cytoplasm as intracellular Ca^{2+} waves (Rooney *et al.* 1989, 1990; Hirata *et al.* 2002). The strength of the extracellular stimulus is primarily encoded in the frequency of $[Ca^{2+}]_c$ oscillations, whereas the rate of $[Ca^{2+}]_c$ rise and amplitude are largely unaffected by hormone concentration (Rooney *et al.* 1989). Perfusing the *ex vivo* rat liver with glucogenic hormones also induces frequency-modulated $[Ca^{2+}]_c$ oscillations within the hepatocytes that have similar spatiotemporal properties to those measured *in vitro* (Robb-Gaspers & Thomas, 1995). In addition, hormone-induced Ca^{2+} increases can propagate into

neighbouring hepatocytes through gap junctions to generate intercellular Ca^{2+} waves. In the continuous presence of subthreshold doses of hormone, the Ca^{2+} responses are asynchronous and only propagate short distances along the hepatic plates prior to dissipating, whereas, at higher concentrations of hormone, the Ca^{2+} increases propagate across entire lobules as spatially organized Ca^{2+} waves. Pharmacological inhibition of gap junction communication or disruption of cell to cell contacts both result in a marked decrease in hormone sensitivity and the reappearance of the asynchronous pattern of Ca^{2+} increases, which do not propagate into neighbouring hepatocytes (Gaspers & Thomas, 2005). Thus, the liver lobule is a functional syncytium, analogous to that in cardiac muscle, although it relies on intracellular Ca^{2+} release rather than membrane depolarization to propagate the signal.

In the present study, electrical stimulation of the sympathetic nerve bundles entering the liver is shown to produce localized $[Ca^{2+}]_c$ increases that are largely confined to the periportal regions of the lobule. The combination of sympathetic stimulation with subthreshold doses of vasopressin delivered systemically via the hepatic portal vein resulted in a synergistic effect between the two stimuli, which amplified the Ca^{2+} responses and converted asynchronous local Ca^{2+} signalling into co-ordinated and spatially organized intercellular Ca^{2+} waves that traversed entire hepatic lobules. The synergism between low levels of vasopressin and sympathetic stimulation produced higher rates of hepatic glucose production. We also examined the effects of glucagon on the ability of vasopressin to induce intercellular Ca^{2+} waves and control hepatic glucose output. Perfusing the liver with physiological doses of glucagon did not induce a $[Ca^{2+}]_c$ response alone but recruited additional hepatocytes to respond to a low dose of vasopressin and hence resulted in larger synchronized intercellular Ca^{2+} waves. The organization of vasopressin-induced intercellular Ca^{2+} waves by glucagon also elicited higher rates of hepatic glucose production compared to vasopressin alone.

Taken together, the results of the present study demonstrate that activation of sympathetic innervation or stimulation of glucagon secretion act to increase the sensitivity of the liver to low levels of circulating hormones such as vasopressin or epinephrine. The net effect is the generation of co-ordinated intercellular Ca^{2+} waves that propagate greater distances through the liver lobule. We conclude that this results from the establishment of an excitable medium generated by subthreshold hormone doses acting on the phosphoinositide signalling cascade, which allows a limited number of pacemaker-like cells to drive intralobular Ca^{2+} waves and, in turn amplifying hepatic glucose production.

Methods

Ethical approval and animals

Animal studies were approved by the Institutional Animal Care and Use Committee at Rutgers, New Jersey Medical School and comply with the ethical principles under which the *Journal of Physiology* operates (Grundy, 2015). Male Sprague–Dawley rats (weighing 200–250 g; Taconic Biosciences, Rensselaer, NY, USA) were housed in ventilated cages under a 12:12 h dark /light cycle in a fully AAALAC (Association for Assessment and Accreditation of Laboratory Animal Care) accredited animal facility. Rats were given *ad libitum* access to rodent chow and water until the day of experiment. Rats were anaesthetized with an I.P. injection of pentobarbital (60 mg kg^{-1}) diluted 1:1 with PBS and vital signs were monitored throughout the procedure. The depth of anaesthesia was assessed by relaxation of muscle tone and a loss of reflex responses to external stimuli. Liver tissue was harvested under a surgical plane of anaesthesia. The organ donor did not recover from surgery.

Reagents

Fura-2/AM, pluronic acid F-127 and fluorescein conjugated-BSA were obtained from Thermo Fisher Scientific (Waltham, MA, USA); bromosulphophthalein was obtained from Fluka (Fluka, Buchs, Switzerland); and hydroxyethyl piperazineethanesulphonic acid (Hepes) and all other chemicals were obtained from Sigma-Aldrich (St Louis, MO, USA).

Heat shock, fraction V BSA was from Roche (Basel , Switzerland). BSA was extensively dialysed against normal saline plus 10 mM Hepes using Spectra/Por 12–14 kDa cut-off dialysis tubing (Thermo Fisher Scientific).

Liver isolation

The livers from anaesthetized (60 mg kg^{-1} body weight Nembutal; Diamondback Drugs, Scottsdale, AZ, USA), fed male Sprague–Dawley rats (weighing 200–250 g; Taconic Biosciences) were perfused *in situ* via the portal vein as described previously (Robb-Gaspers & Thomas, 1995; Gaspers *et al.* 2001). The left and caudate lobes were ligated with silk sutures and surgically removed to increase the loading efficiency of Ca^{2+}-sensitive indicator dyes for confocal imaging (Robb-Gaspers & Thomas, 1995; Gaspers *et al.* 2001). The inferior vena cava was cannulated to permit the recirculation of the perfusate during the dye loading protocol. The perfusion rate was maintained at ~3.5 mL min^{-1} g^{-1} wet weight liver. The perfusion buffer comprised (in mM): 121 NaCl, 25 Hepes (pH 7.4 at 30°C), 5 $NaHCO_3$, 4.7 KCl, 1.2 KH_2PO_4, 1.2 $MgSO_4$, 1.3 $CaCl_2$, 5.5 glucose, 0.5 glutamine, 3 lactate, 0.3 pyruvate, 0.1 tyrosine,

0.2 bromosulphophthalein and 0.1% (w/v) dialysed BSA, equilibrated with 100% O_2. Bromosulphophthalein, an organic anion transport inhibitor, was included to inhibit efflux of Ca^{2+}-sensitive indicator dyes from hepatocytes (Robb-Gaspers & Thomas, 1995; Gaspers *et al.* 2001). After 15 min of initial perfusion, the Ca^{2+}-sensitive indicator dyes were loaded by recirculating 60 mL of the perfusion buffer supplemented with 5 μM fura-2/AM, 0.02% (w/v) pluronic acid F-127 and 2% (w/v) dialysed BSA for 30 min. After the dye loading protocol, the remnant liver was dissected and transferred to a custom built imaging chamber fitted onto the microscope stage to establish an *ex vivo* perfused liver preparation. A description of the imaging chamber and techniques for stabilizing the *ex vivo* perfused liver has been described previously (Robb-Gaspers & Thomas, 1995; Gaspers *et al.* 2001).

Confocal imaging and data analysis

Confocal images were acquired with a Radiance 2002-MP laser scanning multiphoton confocal microscope (Bio-Rad, Hercules, CA, USA) using either 10 × 0.5 NA or 20 × 0.75 NA PlanFluor objectives (Nikon, Tokyo, Japan) and the manufacturer's software. The confocal system was equipped with a 50 mW argon laser and a 10 W Mira/Verdi Ti:sapphire laser from Coherent Inc. (Santa Clara, CA, USA). The Ti:sapphire laser was used for multiphoton excitation of the Ca^{2+}-sensitive indicator, fura-2 and the 488 nm argon laser line was utilized for single photon excitation of mitochondrial flavoproteins. Fura-2 was detected with 810 nm excitation, which only excites the Ca^{2+}-free form of fura-2. Thus, an increase in cytosolic Ca^{2+} corresponds to a decrease in fura-2 fluorescence intensity. In some studies, the electrically-evoked $[Ca^{2+}]_c$ responses were monitored along with the redox state of mitochondrial flavoproteins by combining multiphoton and single photon excitation as described previously (Gaspers & Thomas, 2008). To identify the different lobule zones, a bolus of fluorescein-labelled bovine serum albumin (F-BSA) was injected into the perfusion line just upstream of the liver at the end of each experiment. The appearance of F-BSA fluorescence in the liver sinusoids spaces was monitored using 488 nm argon laser excitation.

Stimulus-induced changes in fura-2 and mitochondrial flavoproteins fluorescence intensities were analysed using in-house bespoke software or algorithms written for ImageJ (NIH, Bethesda, MD, USA). Movements of the liver tissue in the *x,y* direction during data acquisition were corrected using the StackReg plugin for ImageJ (Thevenaz *et al.* 1998).

Confocal images of stimulus-induced increases in Ca^{2+} or mitochondrial flavoprotein redox are presented as the actual fluorescence intensities depicted on a linear grey scale, with the $[Ca^{2+}]_c$ or redox changes at each time point displayed as a coloured overlay. Changes in $[Ca^{2+}]_c$ or mitochondrial flavoproteins were calculated by subtracting sequential time-averaged fluorescence images to obtain a differential image at each point. The intensity of the coloured overlay is proportional to the negative fluorescence change at each point. The difference images were processed with a median filter and a minimum threshold to remove high-frequency noise.

For Ca^{2+} spike analysis, fura-2 fluorescence intensity changes were normalized using $(F/F_0)^{-1}$. The amplitude and spike width at half-peak height were determined using algorithms (Brumer R & Thomas A, unpublished work) written in MATLAB (MathWorks, Natick, MA, USA).

Nerve stimulation

Stimulation of the sympathetic nerve bundles that innervate the liver was achieved by perivascular stimulation around the portal vein and the hepatic artery with an electrical field stimulator. A platinum wire connected to the field stimulator was wrapped around the cannulated portal vein close to the hepatic hilum. Electrical stimulation was performed with a SD9 stimulator (Grass Instrument Company, Quincy, MA, USA) by applying rectangular pulses of 2 ms in duration at 4–20 V and 6–20 Hz. The threshold for $[Ca^{2+}]_c$ response varied between liver preparations and so the absolute stimulation levels were adjusted empirically for each preparation.

Glucose output

The livers from anaesthetized, fed male rats (weighing 200–250 g) were perfused *in situ* through the portal vein and effluent collected from the inferior vena cava as described above. In these experiments, the liver was not dissected from the animal and the glucose concentration in the perfusion buffer was decreased to 1 mM. After 15–30 min of initial perfusion, the effluent was collected for glucose determination. Sympathetic nerve bundles were stimulated using a platinum wire wrapped around the portal vein, as described above, and vasopressin and or glucagon were infused into a mixing chamber inserted into the perfusion line. The glucose concentration of each sample was determined using the Glucose (GO) Assay Kit (GAGO-20; Sigma-Aldrich), which is based on a glucose oxidase/peroxidase reagent linked to a coloured product (o-dianisidine). The intensity of the colour measured at 540 nm was proportional to the glucose concentration of the sample and was calibrated with a standard curve for each experiment. The net hepatic glucose output was determined by subtracting the glucose concentration

in the perfusion buffer from the glucose concentration measured in the effluent.

Statistical analysis

Statistical differences between experimental groups was examined using two-way ANOVA with Bonferroni's multiple-comparisons test or by a two-tailed Student's *t* test when comparing just two groups (Prism; GraphPad Software Inc., San Diego, CA, USA). $P < 0.05$ was considered statistically significant. Data are presented as the mean ± SD for the number of livers or measurements, as indicated where appropriate.

Results

Electrical stimulation elicits $[Ca^{2+}]_c$ signals in hepatocytes of intact perfused liver

Previous studies showed that hormone-induced intercellular $[Ca^{2+}]_c$ waves propagate across the lobules of the intact perfused liver (Robb-Gaspers & Thomas, 1995). These intercellular Ca^{2+} waves typically originate from the periportal zones of the lobule, and this organization persists even when the liver is perfused in a retrograde manner through the hepatic veins (Robb-Gaspers & Thomas, 1995). In the present study, we investigated the role of sympathetic innervation with respect to establishing the spatial pattern of these $[Ca^{2+}]_c$ signals. Sympathetic fibres from the splanchnic nerves innervate the rat liver, mostly in the periportal region of the hepatic lobules (McCuskey, 2004; Yi *et al.* 2010). Therefore, we examined the effect of stimulating these nerves on the initiation and propagation of hepatic $[Ca^{2+}]_c$ signals.

Because the hepatic lobular organization is not easily recognizable during live imaging of Ca^{2+}-sensitive indicator dyes in the intact liver, we defined the areas corresponding to periportal and pericentral regions in the lobules by injecting a bolus of fluorescein-conjugated bovine serum albumin (F-BSA) into the perfusion line after each experiment (Gaspers & Thomas, 2005). Confocal microscopy was used to monitor the time-course of F-BSA fluorescence appearing in the hepatic sinusiods. Periportal zones were identified as the areas where the fluorescence intensity initially increases (Fig. 1*A* and *B*) and pericentral regions were identified as areas where F-BSA subsequently appeared (Fig. 1*C* and *D*; see also the Supporting information, Movie S1). Periportal to venous perfusion times ranged between 3 and 5 s, which is one order of magnitude faster than the fastest intralobular Ca^{2+} waves (see below). F-BSA perfusion was also used as an indication that the liver was properly perfused and that all of the lobules examined were reached equally by the perfusate.

Perfusion of the liver with relatively high concentrations of IP_3-generating hormones initially evokes $[Ca^{2+}]_c$ increases in hepatocytes within the periportal zone followed by a wave of $[Ca^{2+}]_c$ increase that propagates radially through the hepatic plate towards the pericentral regions. Each $[Ca^{2+}]_c$ increase elicited in the initating hepatocytes is organized as an intercellular Ca^{2+} wave and thus these 'pacemaker' cells (Robb-Gaspers & Thomas, 1995; Leite *et al.* 2002) control the spatiotemporal pattern of the Ca^{2+} response for the entire lobule. The images in Fig. 2 (see Supporting information, Movie S1) comprise a representative example of a fura-2/AM loaded rat liver that was perfused with 40 pM vasopressin. Concentrations of vasopressin ≥30 pM are sufficient to induce spatially organized intercellular Ca^{2+} waves that propagate across the entire lobule. As reported previously (Robb-Gaspers & Thomas, 1995), these intralobular $[Ca^{2+}]_c$ waves repeat in a periodic manner in the continuous presence of hormone, equivalent to the hormone-induced $[Ca^{2+}]_c$ oscillations in isolated hepatocytes.

To investigate the potential role of sympathetic innveration in inducing hepatic Ca^{2+} signals, we electrically stimulated the bundles of nerves around the portal vein and hepatic artery of the perfused liver. Field stimulation of hepatic nerve fibres for 5 min triggered $[Ca^{2+}]_c$ increases that spread between hepatocytes and were organized as localized intercellular $[Ca^{2+}]_c$ waves. The electrically-evoked Ca^{2+} responses were similar to the intercellular Ca^{2+} waves induced by perfusion with IP_3-linked hormones, although they were spatially confined to the periportal regions of the liver lobules (Fig. 3; see also the Supporting information, Movie S3). The threshold for inducing Ca^{2+} responses for each liver preparation was determined empirically by varying the intensity and the frequency of the electrical stimulations from 4–20 V and 4–20 Hz. At each suprathreshold stimulation, the Ca^{2+} signal originated in the periportal zones and travelled a short distance towards the pericentral regions of the lobules, although it always terminated without spreading along the full length of the hepatic plates. During the 5 min electrical stimulation protocol, Ca^{2+} responses were not observed in every periportal region and, most often, electrical stimulation yielded a single multicellular Ca^{2+} response rather than the repetitive $[Ca^{2+}]_c$ waves usually observed when the liver was stimulated for longer periods with an IP_3-generating hormone. However, in some cases, the electrical stimulation triggered repetitive $[Ca^{2+}]_c$ events that appeared as restricted multicellular Ca^{2+} bursts in the periportal regions. The images in Fig. 4 (see Supporting information, Movie S4) show an example of two consecutive and spatially restricted $[Ca^{2+}]_c$ waves generating and dissipating in a confined periportal region. The area displayed in Fig. 4 and the corresponding video reflects a collection of images at a higher magnification.

The trace in Fig. 4 is an example of the electrically-evoked $[Ca^{2+}]_c$ spikes in the single hepatocyte highlighted with a green region of interest (ROI).

One of the downstream targets of Ca^{2+} signalling is the activation of mitochondrial metabolism, which can be monitored by recording the fluorescence intensity of matrix flavoproteins. Decreases in fluorescence intensity correlate with a reduction in the FAD/$FADH_2$ redox pair and reflect Ca^{2+}-dependent activation of mitochondrial oxidative metabolism (Scholz *et al.* 1969;

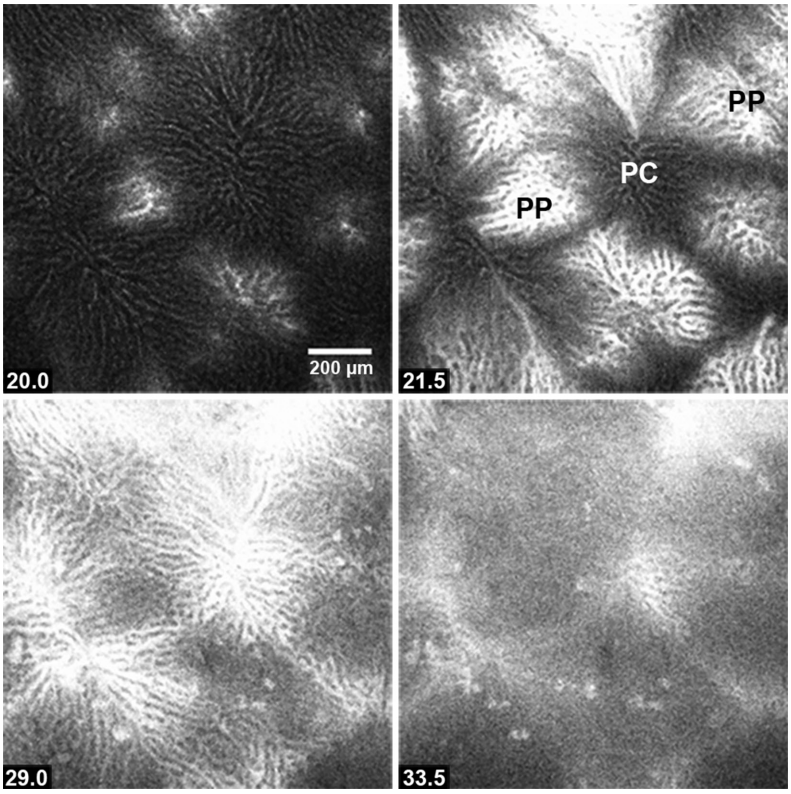

Figure 1. Determination of hepatic lobular zones
Fluorescein-conjugated BSA (100–300 μL of 10 mg mL^{-1} stock) was injected into the perfusion line entering the portal vein prior to the termination of each experiment (see Methods). Periportal (PP) zones were identified as sites where the fluorescence intensity initial increases, whereas pericentral regions (PC) are located where the fluorescein subsequently appears. Time points (s) are shown at the bottom left. The figure corresponds to Movie S1 in the Supporting information.

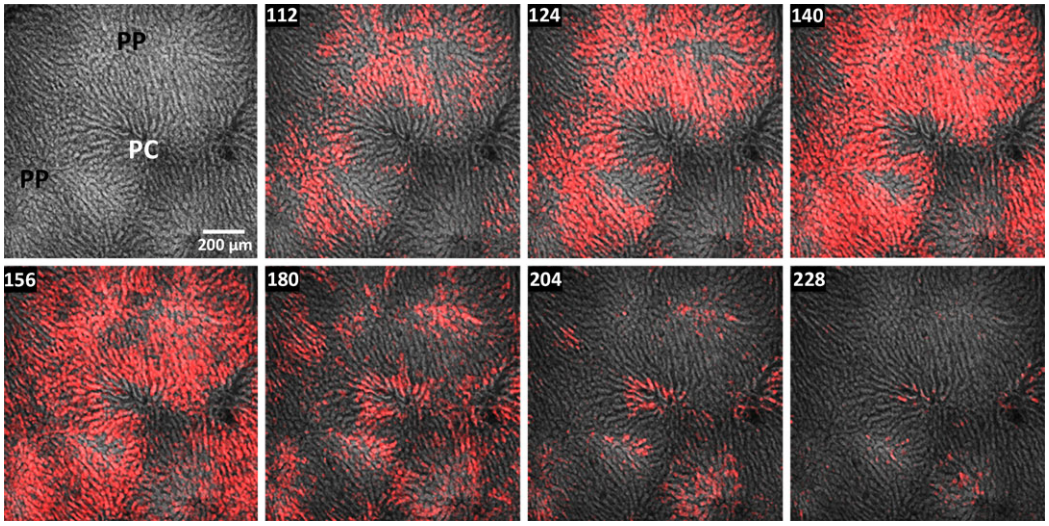

Figure 2. Intercellular $[Ca^{2+}]_c$ waves induced by vasopressin
Fura-2/AM loaded rat liver was perfused with 40 pM vasopressin starting at 68 s. Multiphoton confocal images of fura2 fluorescence are depicted in a linear grey scale and the hormone-induced $[Ca^{2+}]_c$ increases with a red overlay (see Methods). The images show a spatially organized intercellular wave initiated from the periportal region (PP) and propagating into the pericentral zone (PC). The figure corresponds to Movie S2 in the Supporting information. Time points (s) are shown at the top left.

Hajnóczky *et al.* 1995). Electrically-evoked increases in $[Ca^{2+}]_c$ and subsequent changes in the fluorescence of redox-sensitive mitochondrial flavoproteins were simultaneously monitored by combining multiphoton illumination to excite fura-2, together with a single-photon argon laser to excite FAD (Gaspers & Thomas, 2008). Electrical stimulation induced an intercellular $[Ca^{2+}]_c$ wave that propagated from a periportal zone towards the pericentral region (Fig. 5*A*), which was followed by a decrease in the fluorescence intensity of mitochondrial flavoproteins indicating the activation of oxidative metabolism (Fig. 5*B*). The traces in Fig. 5*Ca* show a representative electrically-induced $[Ca^{2+}]_c$ spike (red trace) and reduction in mitochondrial flavoproteins (green trace) in a single hepatocyte within the perfused liver. Similar to responses in isolated cells (Hajnóczky *et al.* 1995), the flavoprotein response lagged slightly behind the $[Ca^{2+}]_i$ increase and had slower rates of rise and decay compared to the Ca^{2+} spike. The traces in Fig. 5*Cb* show the mitochondrial FAD/$FADH_2$ responses in three hepatocytes in-line with the direction of the intercellular Ca^{2+} wave for the coloured ROIs and arrow shown in Fig 5*B*. The results demonstrate that electrical stimulation induces a metabolic response that is spatially organized as an intercellular redox wave, which propagates across the lobule with similar spatiotemporal characteristics as the intercellular Ca^{2+} wave.

Sympathetic electrical stimulation synergizes with and co-ordinates hormone-induced Ca^{2+} responses

We next assessed whether sympathetic stimulation can synergize with low levels of circulating hormones to control the spatiotemporal pattern of Ca^{2+} responses across the hepatic lobule. In rat, basal levels of circulating vasopressin are in the range 2–5 pM and can increase

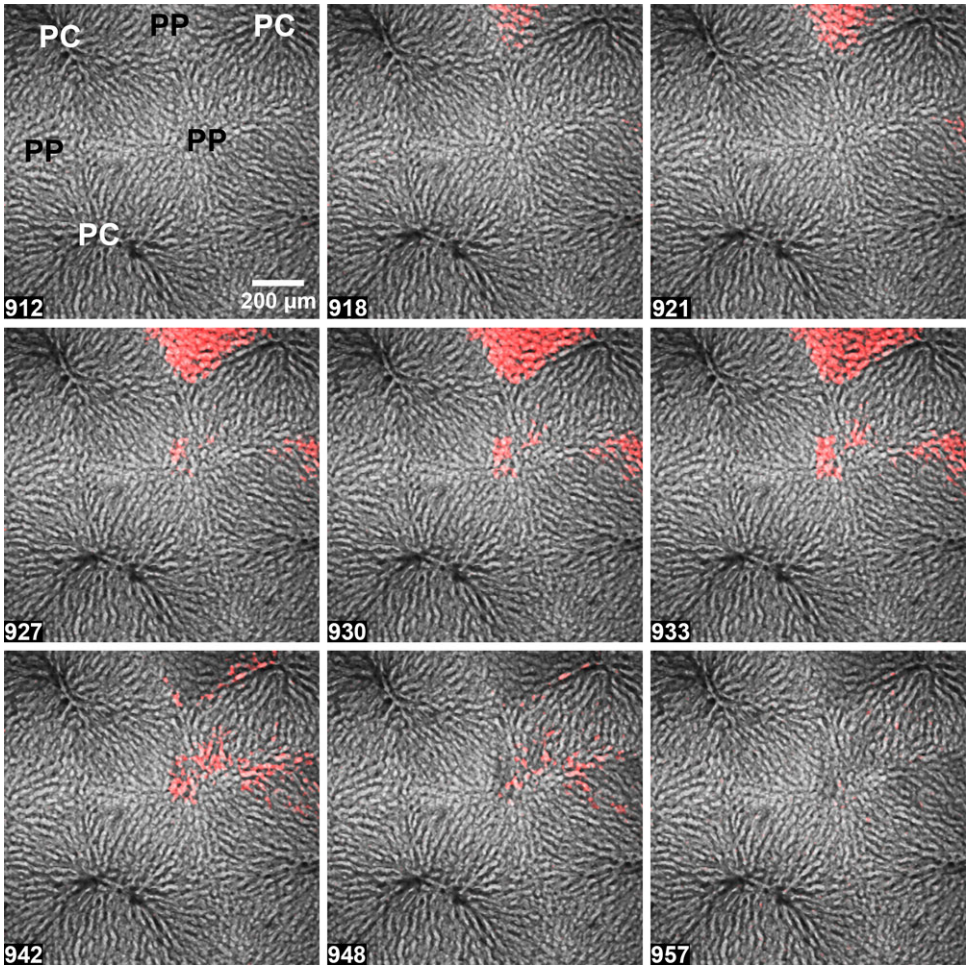

Figure 3. Electrical stimulation elicits localized intercellular Ca^{2+} waves in the intact perfused liver
Hepatic nerve fibres were stimulated for 5 min at 10 V and 10 Hz starting at 912 s. Electrically-induced Ca^{2+} responses were largely confined to the periportal (PP) regions, with only limited propagation towards the pericentral (PC) zones. The figure corresponds to Movie S3 in the Supporting information. The time points (s) are shown at the bottom left.

to 20–30 pM in response to stressful conditions such as prolonged water deprivation or hypoglycaemia (Dunn *et al.* 1973; Baylis & Heath, 1977; Baylis & Robertson, 1980; Fyhrquist *et al.* 1981; Brunner *et al.* 1983). Perfusing the liver with 1–10 pM vasopressin induced an asynchronous pattern of Ca^{2+} spiking in a limited number of hepatocytes, which did not give rise to spatially organized intercellular $[Ca^{2+}]_c$ waves. The red overlay in the confocal image marked 192 in Fig. 6 illustrates the spatially disorganized $[Ca^{2+}]_c$ responses induced by perfusing 10 pM vasopressin (see Supporting information, Movie S5). The data show a few vasopressin-responsive hepatocytes scattered throughout the lobule. Stimulating the sympathetic nerves in the continuous presence of 10 pM vasopressin induced a global $[Ca^{2+}]_c$ response composed of several co-ordinated intercellular Ca^{2+} waves

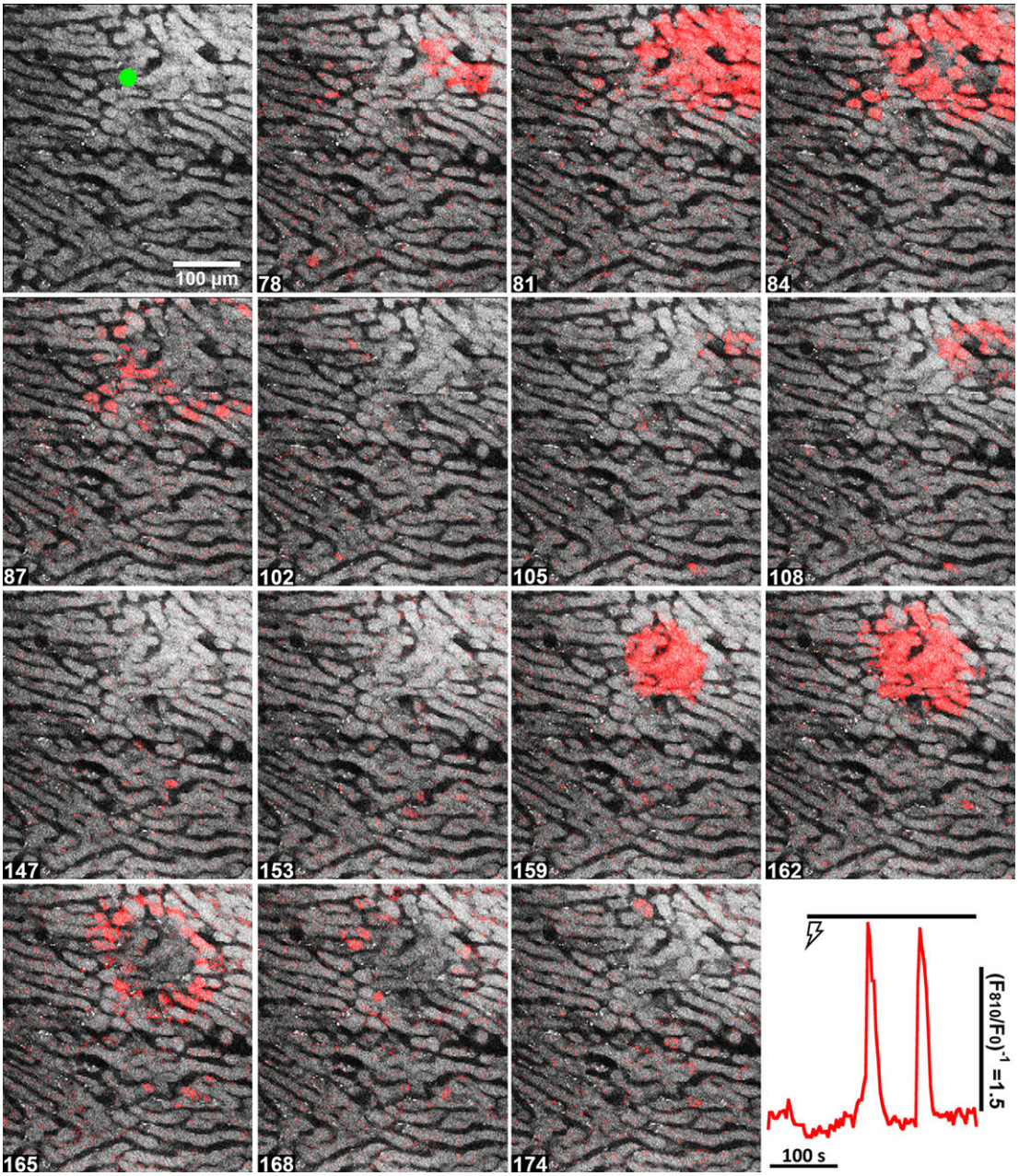

Figure 4. Repetitive localized intercellular Ca^{2+} waves elicited during continuous electrical stimulation of an intact perfused liver
Hepatic nerve fibres were stimulated for 5 min at 4 V and 6 Hz starting at 60 s. The figure corresponds to Movie S4 in the Supporting information. Time points (s) are shown at the bottom left. The trace (bottom right) shows the Ca^{2+} increases induced by electrical stimulation (⚡) in the single hepatocyte highlighted by the green ROI in the top left panel.

that originated around the periportal regions and spread across the entire field of view (Fig. 6, panels 216–303). The $[Ca^{2+}]_i$ increases following electrical stimulation in the presence of vasopressin are shown in Fig. 6*B* for three hepatocytes, highlighted with respect to the coloured ROIs in the initial image of Fig. 6*A*, showing propagation of an intercellular Ca^{2+} wave across the lobule. These Ca^{2+} responses are reminiscent of the intercellular Ca^{2+} waves induced by higher doses of vasopressin in the absence of electrical stimulation (Fig. 2). In some experiments, when the electrical stimulation was sustained for a sufficient length, the combination of electrical stimulation and subthreshold vasopressin induced repetitive Ca^{2+} waves across the entire lobule. Electrical stimulation also triggered lobular Ca^{2+} waves even when the initial perfusion of vasopressin did not induce any $[Ca^{2+}]_c$ response (not shown). In the absence of hormone, electrical stimulation never evoked a sustained rise in $[Ca^{2+}]_c$ or produced intercellular Ca^{2+} waves that traversed across entire lobules.

The role of α_1-adrenergic receptors in the Ca^{2+} responses evoked by electrical stimulation was confirmed by including the α-blocker prazosin in the perfusate buffer. As expected, perfusing the liver with prazosin did not inhibit the asynchronous Ca^{2+} spikes induced by subthreshold concentrations of vasopressin (Fig. 7*B*). However, prazosin treatment suppressed the synergy between electrical stimulation and the Ca^{2+} increases induced by low vasopressin stimulation (Fig. 7). The prazosin concentration used in this experiment was sufficient to block Ca^{2+} oscillations induced by phenylephrine, an α_1-adrenergic receptor agonist, in both periportal and pericentral hepatocytes (not shown). These data are consistent with electrical stimulation evoking the release of norepinephrine from sympathetic nerve fibres, which in turn stimulates α_1-adrenergic receptors on hepatocytes to co-ordinate and potentiate the Ca^{2+} waves across the liver lobule.

The $[Ca^{2+}]_c$ responses in individual hepatocytes from the experiments shown in Figs 4 and 6 were aligned with the rising phase of the Ca^{2+} transient to generate the mean $[Ca^{2+}]_c$ spike induced by electrical stimulation, subthreshold vasopressin or vasopressin plus electrical stimulation (Fig. 8*A* and *B*). The experimental protocols described in Figs 4 and 6 were also repeated in additional liver preparations, and summary data are shown with black symbols in Fig. 8*C–E*. In some studies, electrical stimulation was carried out both before and after vasopressin perfusion in the same liver preparation. Sympathetic nerve bundles were stimulated for 5 min, followed by 8 min of recovery and then perfusion with 10 pM vasopressin for an additional 8 min, followed by a second 5 min electrical stimulation. Summary data for these $[Ca^{2+}]_c$ experiments are shown with coloured symbols in Fig. 8*C–E*.

Consistent with our isolated hepatocyte studies (Rooney *et al.* 1990), there was no difference in the amplitude of Ca^{2+} increases induced by any of the stimuli (Fig. 8*C*). The width or duration of the individual cell $[Ca^{2+}]_c$ spikes calculated at half-maximum was the shortest for electrically-evoked Ca^{2+} transients, and this parameter was significantly longer for vasopressin and even more prolonged in the vasopressin plus electrical stimulation group (Fig. 8*D*). The shape of

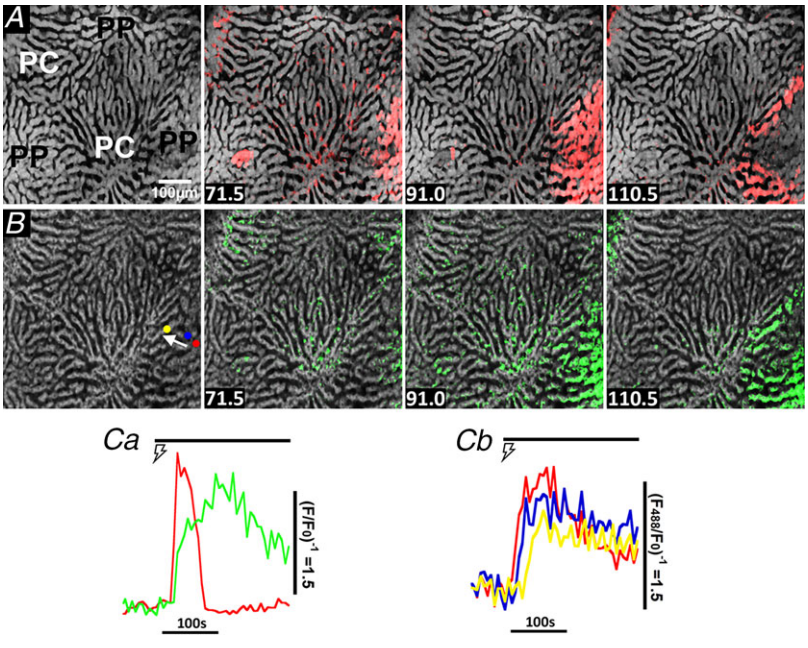

Figure 5. Electrically-evoked $[Ca^{2+}]_c$ and mitochondrial flavoprotein responses in the intact perfused liver
Fura-2/AM loaded liver was sequentially illuminated with 810 nm and 488 nm excitation to monitor cytosolic Ca^{2+} (*A*, upper row of images) and the redox state of mitochondrial flavoproteins (*B*, lower row of images), respectively. Hepatic nerve fibres were stimulated for 5 min at 4 V and 10 Hz starting at 33 s, which induced a periportal (PP) Ca^{2+} wave (red overlay) that was followed by a reduction in mitochondrial flavoproteins (green overlay). Time points (s) are shown at the bottom left. *Ca*, single cell trace of an electrically-induced (⚡) Ca^{2+} spike (red) and corresponding reduction in mitochondrial flavoproteins (green). *Cb*, traces are electrically-induced mitochondrial flavoprotein responses in three hepatocytes highlighted by the coloured regions of interest shown in (*B*) and chosen to be in-line with the Ca^{2+} wave propagation pathway (white arrow).

the electrically-induced $[Ca^{2+}]_c$ spikes was similar to $[Ca^{2+}]_c$ transients induced by the α_1-adrenergic agonist phenylephrine in isolated hepatocytes and, similarly, the broader $[Ca^{2+}]_c$ spikes with vasopressin in hepatocytes of the perfused liver were comparable to those observed with this hormone in isolated hepatocyte preparations (Rooney *et al.* 1989). However, in the presence of vasopressin, electrical stimulation gave rise to $[Ca^{2+}]_c$ transients with even slower rates of decline. This increase in Ca^{2+} spike width does not appear to be caused by a shift in the sensitivity of the liver to vasopressin because the duration and amplitude of $[Ca^{2+}]_c$ spikes induced by higher concentrations of vasopressin (30–100 pM) that result in co-ordinated intercellular Ca^{2+} waves (Fig. 2) were not different from those induced by 10 pM vasopressin. The width at half-height was 34 ± 5.0 s and 33.5 ± 5.0 s ($P > 0.05$), whereas the amplitude of the spike was 0.32 ± 0.1 $\Delta F/F$ and 0.49 ± 0.2 $\Delta F/F$ ($P > 0.05$) for the 10 pM and ≥30 pM vasopressin groups, respectively (mean ± SD, $n = 7$ to 10 liver preparations and 300–400 hepatocytes analysed per hormone dose).

The percentage of the field of view that displayed a $[Ca^{2+}]_c$ increase during the initial 5 min of stimulation was calculated for each stimulus protocol. The average percentage of the field responding to electrical stimulation alone or to 10 pM vasopressin was comparable reaching 15 ± 16.0% or 15 ± 12.0%, respectively. By contrast, co-stimulation acted synergistically to increase the percentage of responding cells to 82 ± 23% (Fig. 8*E*).

In summary, these findings demonstrate that activation of hepatic sympathetic innervation induces localized $[Ca^{2+}]_c$ increases in a subset of periportal hepatocytes, which do not propagate across the hepatic lobule as intercellular Ca^{2+} waves. However, the same electrical stimulus intensity can amplify asynchronous $[Ca^{2+}]_c$ increases induced by subthreshold doses of vasopressin into co-ordinated intercellular Ca^{2+} waves that propagate across entire hepatic lobules. In the absence of hormone, electrical stimulation produces a Ca^{2+} spike that is

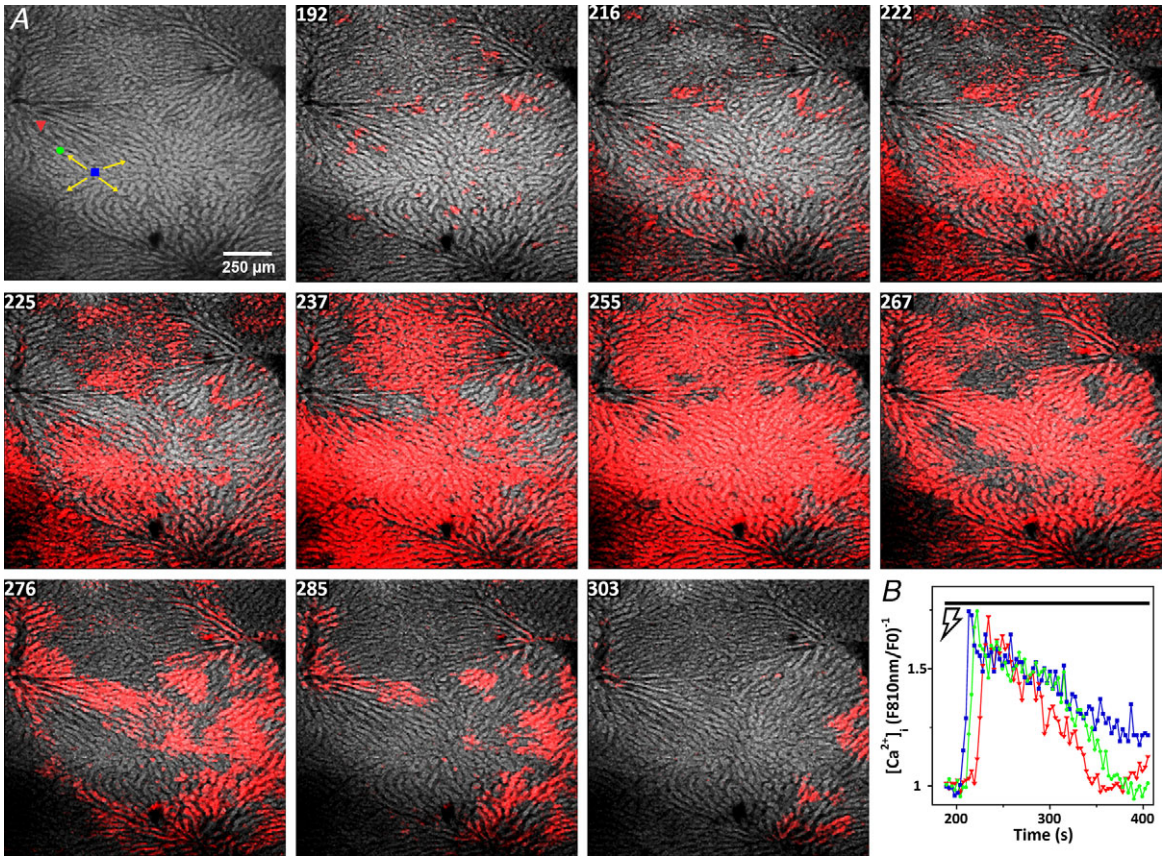

Figure 6. Electrical stimulation synergizes with the Ca^{2+}-responses induced by low concentrations of vasopressin
Fura-2/AM loaded liver was perfused with a subthreshold dose of vasopressin (10 pM, panels 150–192 s) prior to stimulating the hepatic nerve fibres at 4 V and 4 Hz starting at 195 s. Time is indicated (s). The figure corresponds to Movie S5 in the Supporting information. *A*, blue, green and red ROIs represent three hepatocytes along a hepatic plate from the periportal to pericentral regions, respectively. *B*, time courses of the electrically-induced $[Ca^{2+}]_c$ increases in the ROIs.

kinetically similar to those induced by α_1-adrenergic agonists, consistent with the release of norepinephrine from the liver after stimulation of the portal nerve plexus (Hartmann *et al.* 1982; Gardemann *et al.* 1987). In the presence of vasopressin, however, electrically-evoked Ca^{2+} spikes are significantly longer in duration even in hepatocytes that had not previously responded to the vasopressin. These data are consistent with the hypothesis that subthreshold stimulation by systemic perfusion with vasopressin establishes an excitable medium (Lechleiter *et al.* 1991) in the liver tissue as a result of the subthreshold elevation of intracellular IP_3, which can then be triggered to generate translobular Ca^{2+} waves by a stronger but local stimulation arising from the sympathetic innervation.

Vasopressin-induced intercellular Ca^{2+} waves are potentiated by low levels of glucagon

Glucagon is another major hormonal regulator of hepatic glucose production. Glucagon receptors primarily couple to adenylyl cyclase to increase cAMP and activate protein kinase A (PKA), leading to stimulation of glycogenolysis and gluconeogenesis (Jiang & Zhang, 2003). PKA was shown to phosphorylate IP_3 receptors and sensitize IP_3-induced Ca^{2+} release from the endoplasmic reticulum (Burgess *et al.* 1991; Bird *et al.* 1993; Hajnóczky *et al.* 1993; Rooney *et al.* 1996; Wagner *et al.* 2008; Betzenhauser *et al.* 2009; Wang *et al.* 2012; Taylor, 2017). We therefore investigated whether glucagon could potentiate intercellular Ca^{2+} waves induced by low levels of IP_3-forming hormones (Fig. 9). Perfusion of rat livers with physiological levels of glucagon (5–60 pM) (Emmanouel *et al.* 1978; Wewer Albrechtsen *et al.* 2016) had no effect on $[Ca^{2+}]_c$ in the absence of IP_3-linked hormones, whereas supraphysiological concentrations of glucagon (1–50 nM) can induce asynchronous $[Ca^{2+}]_c$ increases, although these responses are still not organized as intercellular Ca^{2+} waves (Gaspers & Thomas, 2005). The confocal images in Fig. 9*A* show vasopressin-induced $[Ca^{2+}]_c$ signals in the absence and presence of 5 pM glucagon. Vasopressin perfusion evoked local intercellular Ca^{2+} waves that spread through a limited number of cells mostly in the periportal zone and did not recruit all of the neighbouring cells, nor penetrate into the pericentral zone. However, in the presence of subthreshold glucagon, the vasopressin-induced

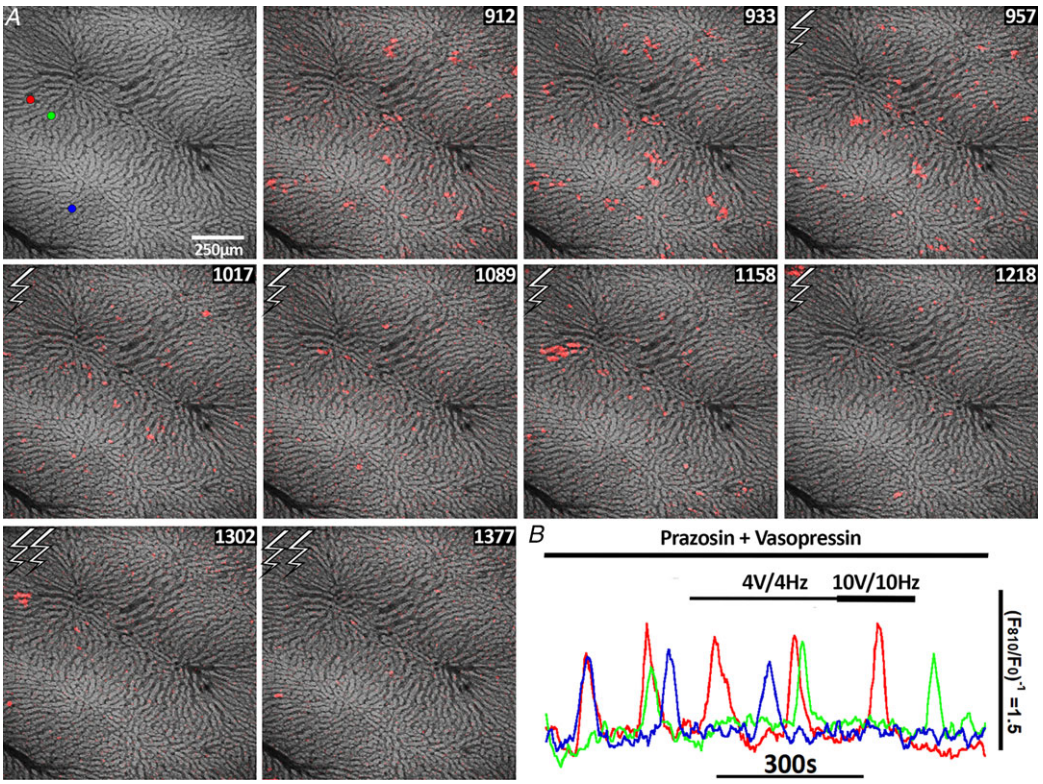

Figure 7. Prazosin suppresses the synergy between electrical stimulation and low concentrations of vasopressin
Liver was perfused with 200 nM prazosin for 25 min followed by perfusion with a subthreshold concentration of vasopressin (7.5 pM) plus prazosin (panels 912–933). Hepatic nerve fibres were stimulated at 4 V and 4 Hz between in panels 957–1218 and 10 V and 10 Hz in panels 1302–1377. *A*, red, green and blue ROIs show the position of three cells for which the Ca^{2+} responses are shown in (*B*). *B*, time courses of the $[Ca^{2+}]_c$ responses in the ROIs.

Ca^{2+} responses recruited essentially all of the previously unresponsive hepatocytes and became organized as a full propagating intercellular Ca^{2+} waves throughout the hepatic lobule. Thus, it appears that glucagon can enhance the excitability of the lobular syncytium of hepatocytes, presumably by PKA-dependent phosphorylation of the IP_3 receptor Ca^{2+} channel, and, in this way, decrease the threshold for low levels of vasopressin to elicit full intralobular Ca^{2+} waves.

In a separate experimental paradigm, the liver was sequentially perfused with 10 and then 30 pM vasopressin (Fig. 9*B* and *D*). Vasopressin was then washed out for 30 min and the liver was challenged with 5 pM glucagon prior to vasopressin (Fig. 9*C* and *E*). As noted above, glucagon alone did not increase $[Ca^{2+}]_c$ but caused a marked increase in the sensitivity of the liver to low-dose vasopressin stimulation. Treatment with glucagon increased the frequency of vasopressin-induced Ca^{2+} spiking (compare Fig. 9*B* and *C*) and the percentage of hepatocytes responding to vasopressin stimulation as evident by the larger and faster increases in the mean Ca^{2+} traces (compare Fig. 9*D* and *E*).

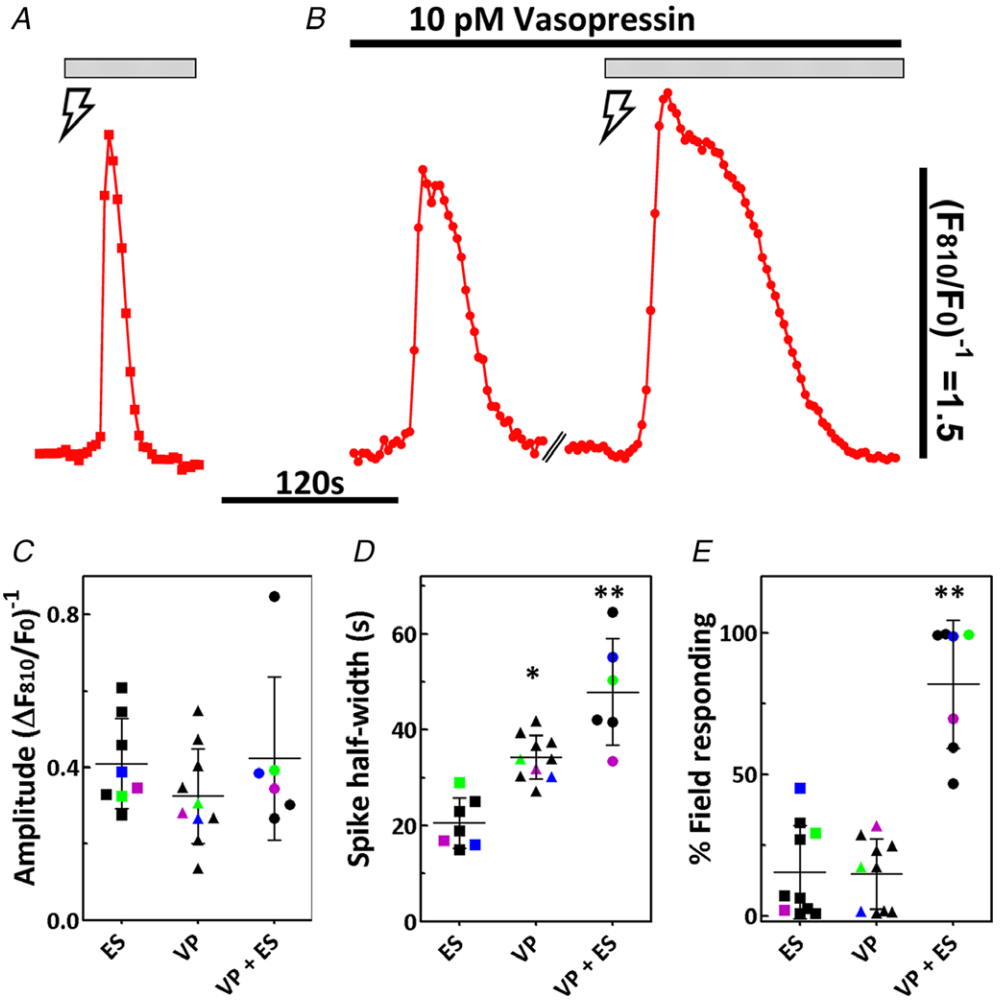

Figure 8. Summary of Ca^{2+}-responses induced by electrical and hormonal stimuli in the perfused liver
A and *B*, Stimulus-induced Ca^{2+} spikes from experiments shown in Figs 4 and 6 were aligned to the rising phase of the Ca^{2+} transient. Traces are averaged Ca^{2+} transients induced by (*A*) electrical stimulation (⚡) or (*B*) vasopressin stimulation followed by vasopressin plus electrical stimulation (⚡); n = 16–41 cells per condition. Bars above traces indicate the duration of the stimulus and broken line indicates a gap in time series. Summary data showing (*C*) Ca^{2+} spike amplitude and (*D*) spike width calculated at half-height. Ca^{2+} spikes were induced by electrical stimulation (ES; 4 V, 4 Hz), perfusion with 10 pM vasopressin (VP) or vasopressin plus electrical stimulation (VP + ES). *E*, percentage of the field responding with an increase in $[Ca^{2+}]_c$ that occurred within 5 min after commencing the indicated stimulus. Scatter plots are the mean ± SD with each symbol representing data from a separate liver, n = 6–10 liver preparations and 150–300 hepatocytes analysed per stimulus. The blue, green and purple symbols show data from the same liver preparation put through all three sequential stimuli. ∗Significantly different compared to ES, **Significantly different compared to ES or VP; $P < 0.05$; one-way ANOVA with a *post hoc* Bonferroni test.

Hepatic glucose production is increased in parallel with the co-ordination of hormone-induced intercellular Ca^{2+} waves

The Ca^{2+} imaging studies indicate that both electrical stimulation and glucagon can synergize with low levels of vasopressin to strengthen the $[Ca^{2+}]_c$ signal and facilitate intercellular Ca^{2+} waves that propagate across the entire hepatic lobule. In these experiments, we investigated whether this synergism at the level of Ca^{2+} signalling provides a mechanism to regulate hepatic glucose production.

Previous studies have shown that perfusing the liver with relatively high concentrations of vasopressin induces glycogen degradation and increases hepatic glucose output (Hems & Whitton, 1973; Garrison *et al.* 1979; Exton, 1987). Therefore, we carried out dose–response studies aiming to determine the threshold and sensitivity of the liver to vasopressin-induced glucose mobilization. The liver was perfused with increasing concentrations of vasopressin from 10 pM to 1 nM and the net formation of glucose by the liver was determined (see Methods). Vasopressin concentrations ≥30 pM stimulated a net increase in hepatic glucose output, whereas 10 pM vasopressin had essentially no effect on glucose mobilization (Fig. 10*A*). Thus, 10 pM vasopressin is at or slightly lower than the threshold concentration to stimulate glucose mobilization, which is consistent with the threshold concentration observed for inducing $[Ca^{2+}]_c$ increases in the perfused liver (Fig. 6).

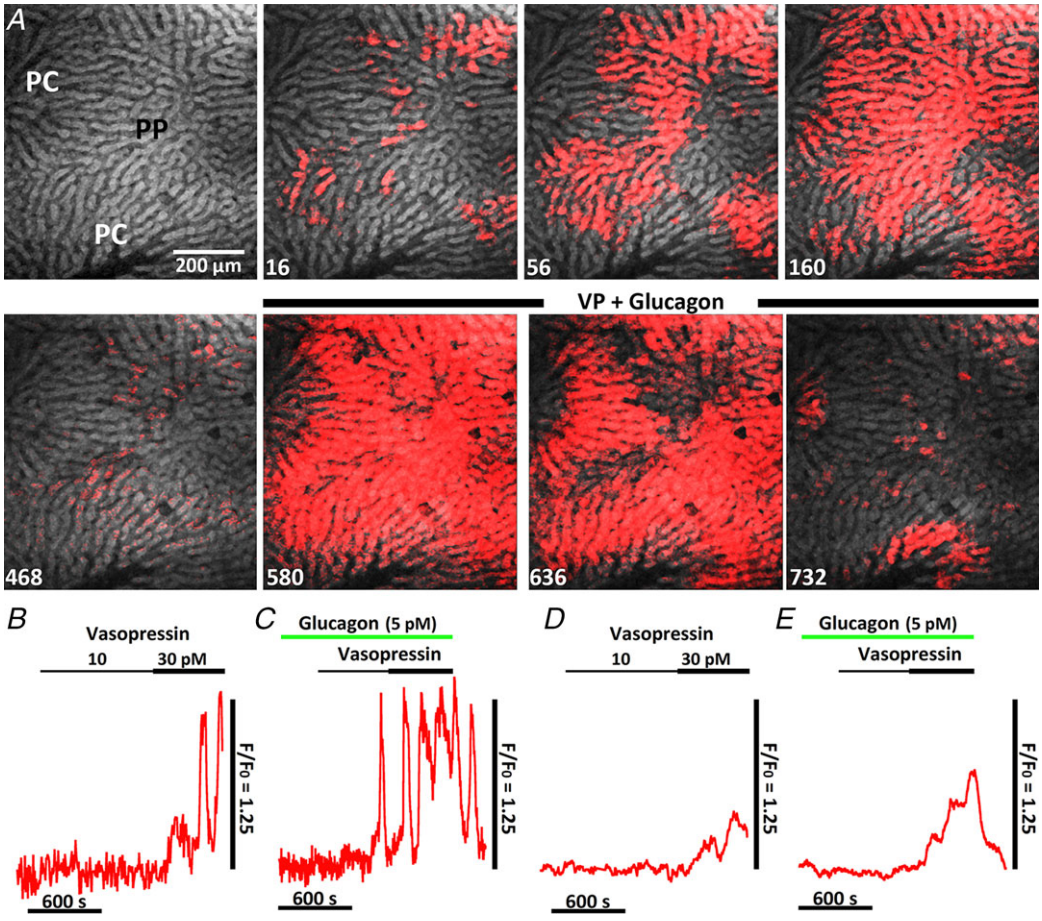

Figure 9. Effect of subthreshold glucagon on vasopressin-induced intercellular Ca^{2+} waves in the perfused liver
A, initial panel shows a confocal image of fura-2 fluorescence depicted in linear grey scale with the periportal (PP) and pericentral (PC) zones identified (see Methods). Time points (s) after vasopressin (30 pM) reaches the liver are shown at the bottom left (upper row). The liver was then co-infused with vasopressin plus glucagon (5 pM) starting at 472 s (lower row). *B–E*, liver was sequentially perfused with increasing vasopressin concentrations, as indicated, and then, following a 30 min washout, the liver was challenged with 5 pM glucagon prior to and throughout vasopressin perfusion. Traces are the hormone-induced Ca^{2+} increases in a single hepatocyte in the absence (*B*) and presence of glucagon (*C*), or the mean Ca^{2+} increases in the absence (*D*) and presence of glucagon (*E*); more than 300 hepatocytes were used to construct the mean Ca^{2+} traces. Similar results were obtained in a second liver preparation.

To investigate the effect of sympathetic stimulation on the glucose response to subthreshold levels of vasopressin, livers were electrically stimulated for 2 min starting at a frequency of 2 Hz and 10 V and then the frequency of stimulation was increased to 5 Hz and 10 Hz with 5 min recovery periods between each stimulation. Previous studies have shown that norepinephrine release is maximally stimulated at 10 Hz (Sannemann *et al.* 1986). The black trace in Fig. 10*B* shows a small increase in hepatic glucose release with 2 Hz stimulation, which increased at higher stimulation frequencies (Fig. 10*C*). In parallel studies, livers were continuously perfused with 10 pM vasopressin starting 5 min prior to the electrical stimulation protocol and the hormone remained present throughout the duration of the experiment. The red trace in Fig. 10*B* shows that 10 pM vasopressin, alone, did not alter glucose output but dramatically enhanced glucose output in response to electrical stimulation, particularly at the lowest frequency of stimulation (i.e. 2 Hz). The amplitude of each glucose peak minus its respective baseline value was determined for each stimulation frequency. These data show that, in the presence of vasopressin, electrical stimulation at 2 Hz triggers a more than 3-fold increase in hepatic glucose production compared to the electrical stimulation alone (Fig. 10*C*).

The norepinephrine released by electrical stimulation could act through both α and β-adrenergic receptors, which raises the possibility that β-adrenergic activation could increase hepatic glucose production via the cAMP/PKA pathway, similar to the actions of glucagon on liver. To test whether β-adrenergic receptors were involved, livers were perfused with vasopressin and 10 μM

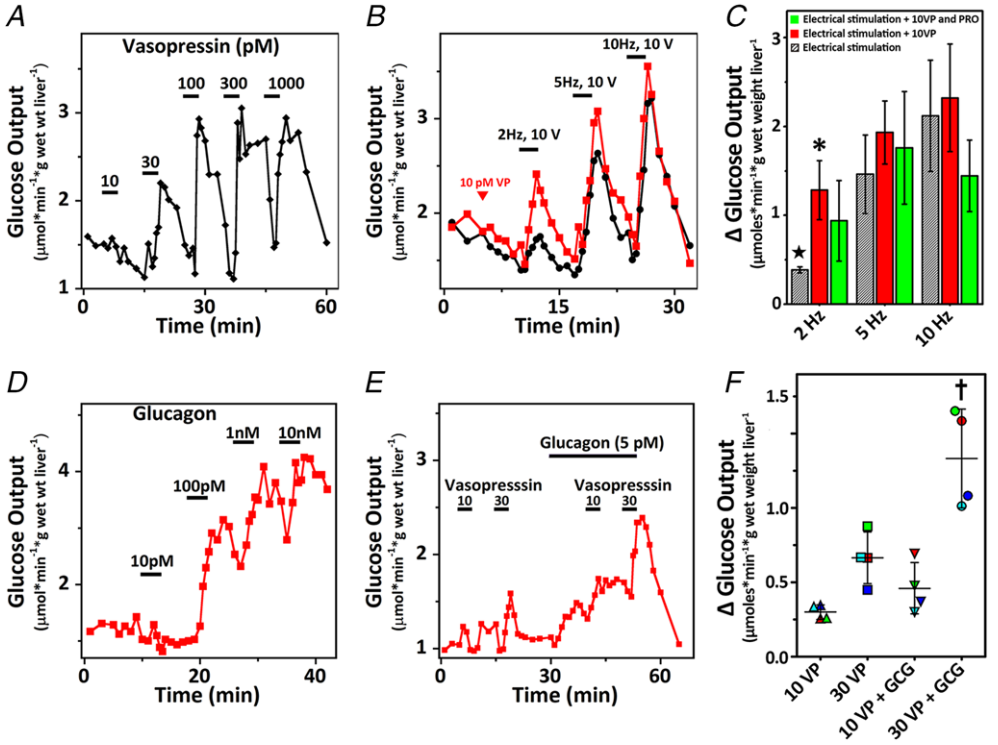

Figure 10. Regulation of hepatic glucose production by stimuli that potentiate intercellular Ca^{2+} waves
A, average hepatic glucose output induced by the indicated concentrations of vasopressin ($n = 3$ livers). *B*, average hepatic glucose output in response to increasing intensity of electrical stimulation in the absence (black trace) or presence (red trace) of 10 pM vasopressin (VP) ($n = 4$ livers). Stimulus and duration are indicated by the horizontal bars. *C*, summary data for electrically-induced changes in hepatic glucose production alone (hatched bars) in the presence of 10 pM vasopressin (red bars) or in the presence of vasopressin and 10 μM propranolol (PRO). ΔGlucose is the peak stimulus-induced increase in glucose production minus its respective baseline. Data are the mean ± SD, $n = 4$–5 livers per group. *D*, hepatic glucose output induced by increasing concentrations of glucagon. Trace is a representative response. *E*, livers were perfused with 10 and 30 pM vasopressin where indicated by the bars and following a washout period the hormone stimulation protocol was repeated in the presence of 5 pM glucagon. Trace is the average glucose output from four livers. *F*, summary data for the amplitude of vasopressin-induced glucose output minus the baseline values in the absence or presence of glucagon (GCG). Symbols with alike colours are glucose measurements from the same liver. The mean ± SD is also shown, $n = 4$ livers. Statistical significance was calculated using two-way ANOVA with Bonferroni's multiple-comparisons test; $^{*}P < 0.05$ *vs*. 2 Hz electrical stimulation alone; $^{\star}P < 0.01$ *vs*. 5 Hz and 10 Hz electrical stimulation alone; $^{\dagger}P < 0.01$ *vs*. other hormone combinations.

propranolol, a β-adrenergic blocker, for 5 min prior to starting the electrical stimulation protocol. Propranolol treatment had a tendency to lower glucose output induced by the highest level of electrical stimulation (10 Hz), although this decrease did not reach significance (Fig. 10*C*, green bars). These results are consistent with previous studies (Hartmann *et al.* 1982; Ulken *et al.* 1991) and suggest that norepinephrine acts primarily through α_1-adrenergic receptors to stimulate hepatic glucose output.

Glucagon concentrations $\leq$10 pM did not induce a measurable increase in hepatic glucose output ($n = 2$ livers) (Fig. 10*D*) in the absence of other stimuli. Higher levels of glucagon dose-dependently increased hepatic glucose production, with a maximal response at 1–10 nM. Physiological levels of glucagon typically fall in the range 5–60 pM (Emmanouel *et al.* 1978; Wewer Albrechtsen *et al.* 2016). The trace in Fig. 10*E* shows the average glucose output in response to perfusing livers with picomolar concentrations of vasopressin in the absence and presence of 5 pM glucagon. These low concentrations of vasopressin in the presence of subthreshold glucagon elicited increased rates of hepatic glucose output compared to vasopressin alone (Fig. 10*F*). Thus, perfusing the liver with vasopressin and glucagon potentiated the propagation of intercellular Ca^{2+} waves (Fig. 9*A*) and this co-stimulation protocol was also more potent in increasing hepatic glucose production compared to either hormone treatment alone. These data indicate that the rates of hepatic glucose production correlate with the extent that hormone-induced Ca^{2+} waves spread across the hepatic lobule, and highlight the importance of these Ca^{2+} waves with respect to recruiting all available hepatocytes to deliver a full metabolic response.

Discussion

Central control of hepatic glucose production originates in the hypothalamus and is mediated by direct sympathetic innervation of the liver, as well as by regulation of pancreatic and adrenal endocrine outputs. Norepinephrine released by sympathetic nerve terminals in the periportal zone acts on hepatic α_1-adrenergic receptors to increase $[Ca^{2+}]_c$, with essentially no actions on ß-adrenergic receptors or cAMP (Hartmann *et al.* 1982; Balle *et al.* 1987). The key finding from the present study is that sympathetic input can act synergistically with physiological and subthreshold levels of systemic hormones to convert asynchronous localized $[Ca^{2+}]_c$ responses into co-ordinated intercellular Ca^{2+} waves that spread throughout the hepatic lobule. Importantly, only this synergistic interaction between multiple inputs can recruit all of the hepatocytes in the lobule and give rise to the full metabolic output of the liver at physiological hormone levels.

Stimulation of the sympathetic efferent nerves in *ex vivo* perfused livers elicited a $[Ca^{2+}]_c$ increase in a small number of hepatocytes within the periportal zone. This localized Ca^{2+} response may reflect the fact that norepinephrine-containing sympathetic nerve fibres are predominately localized to the portal triad, with little intralobular innervation (McCuskey, 2004; Yi *et al.* 2010). The spatiotemporal organization of the $[Ca^{2+}]_c$ responses were completely different when the hepatic nerve bundles were electrically stimulated in the presence of low concentrations of an IP_3-generating hormone. The conditions used here mimic the *in vivo* situation where the release of sympathetic neurotransmitters occurs when circulating hormone levels, such as epinephrine and vasopressin, are typically maintained at tonic subthreshold levels. In this context, it is noteworthy that studies are often carried out using relatively high concentrations of hormones (i.e. in the nanomolar to micromolar range) that are not normally encountered *in vivo*. Moreover, isolated hepatocytes are less sensitive to hormones than hepatocytes in the intact liver, perhaps because of the importance of intercellular communication of signals in establishing hormone sensitivity, although loss of receptor expression may also play a role.

In the present study, we focused on vasopressin as the systemic hormone instead of epinephrine because vasopressin activates hepatic metabolism through Ca^{2+}-dependent mechanisms that do not involve cAMP or PKA (Garrison *et al.* 1979). When livers were perfused with vasopressin at concentrations ~2-fold higher than the basal values measured in peripheral blood (Dunn *et al.* 1973; Fyhrquist *et al.* 1981; Brunner *et al.* 1983), this only induced sporadic asynchronous Ca^{2+} spikes in a small fraction of hepatocytes. The strong co-operative effect between vasopressin and sympathetic activation converted these two weak Ca^{2+}-mobilizing stimuli into well-organized $[Ca^{2+}]_c$ increases, which began in the periportal zone and propagated throughout the entire functional units of the liver. Both vasopressin V1a and α_1-adenergric receptors display lobular zonation with the highest densities in pericentral hepatocytes, resulting in a perivenous to periportal receptor gradient (Ostrowski *et al.* 1993; Nathanson *et al.* 1995; Clair *et al.* 2003). Nevertheless, the physiological levels of stimuli used in the present study consistently induced intercellular Ca^{2+} waves that propagated in a direction opposite to the receptor gradient. Thus, the distribution of hormone receptors along the hepatic plate cannot readily explain the propagation direction of intercellular Ca^{2+} waves. It should be noted that we routinely define the periportal and pericentral zones by monitoring the pathway of a cell impermeant fluorescent marker through the lobule.

We have demonstrated that the propagation of intercellular Ca^{2+} waves requires gap junction communication and also that the spread of Ca^{2+} waves occurs at rates

significantly slower than perfusion flow (Robb-Gaspers & Thomas, 1995; Gaspers & Thomas, 2005). Moreover, intercellular Ca^{2+} waves are not self-regenerating but, instead, require the continuous presence of the hormone or elevated IP_3 to spread throughout the entire lobule (Gaspers & Thomas, 2005). There are several possible mechanisms that could explain the interaction between the activation of sympathetic nerves and circulating hormones at the level of intercellular Ca^{2+} waves. Perfusing with low of levels vasopressin is expected to elevate intracellular IP_3 to subthreshold levels throughout the tissue, which would create an excitable state of the IP_3 receptor Ca^{2+} channels in all cells. Under these conditions, the locally limited $[Ca^{2+}]_c$ increases in a small number of hepatocytes that respond directly to sympathetic activation could act as pacemaker-like cells. These sympathetically-activated pacemaker cells would then recruit neighbouring hepatocytes (already sensitized by subthreshold vasopressin) by diffusion of Ca^{2+} and/or IP_3 through gap junctions to trigger a Ca^{2+} response that regenerates from cell to cell along the hepatic plates. This relies on the positive feedback effects of Ca^{2+} on IP_3 receptors and IP_3 generation in a cross-coupling mechanism, which gives rise to robust full strength $[Ca^{2+}]_c$ spikes, as we have reported previously in isolated hepatocytes (Gaspers *et al.* 2014). This process is somewhat analogous to the proposed 'excitable medium' underling spiral Ca^{2+} waves in *Xenopus* oocytes in the presence of submaximal IP_3 (Lechleiter *et al.* 1991; Atri *et al.* 1993; Clapham, 1995), except, in the liver, the excitable medium is composed of a lobular syncytium of hepatocytes.

A feature of the synergistic interaction between sympathetic stimulation and systemic vasopressin action is the broadening of the individual $[Ca^{2+}]_c$ transients that occurs under these conditions, as assessed at the level of individual cells within the liver (Fig. 8). It is well established that different agonists give rise to $[Ca^{2+}]_c$ oscillations with distinct agonist-specific kinetic properties in hepatocytes and also that vasopressin-induced $[Ca^{2+}]_c$ transients are invariably prolonged relative to those elicited by α -adrenergic agonists (Woods *et al.* 1987; Rooney *et al.* 1989; Bartlett *et al.* 2014). Although the mechanism underlying these agonist-specific Ca^{2+} kinetics remains to be determined, it is not surprising that the $[Ca^{2+}]_c$ transients induced by combined sympathetic stimulation and vasopressin perfusion more closely resemble the systemically-delivered vasopressin. Nevertheless, the $[Ca^{2+}]_c$ transients with combined stimulation appear to be even more prolonged than with vasopressin alone. One explanation for this might be found in the positive feedback of Ca^{2+} on IP_3 formation that underlies the cross-coupling model for $[Ca^{2+}]_c$ oscillations (Gaspers *et al.* 2014). Thus, in the intact liver, permeation of Ca^{2+} and IP_3 through gap junctions could prolong the $[Ca^{2+}]_c$ transients by enhancing the magnitude and extending the duration of these signals, with the neighbouring cells effectively acting as temporal buffers of Ca^{2+} and/or IP_3 analogous to the effects of IP_3 buffers in isolated hepatocytes (Gaspers *et al.* 2014). Significantly, the longer lasting $[Ca^{2+}]_c$ transients observed with the combination of vasopressin plus electrical stimulation are also expected to enhance the metabolic output of the liver compared to either stimulus alone.

The synergistic regulation of hepatic Ca^{2+} signalling was not limited to sympathetic stimulation and was also replicated with low levels of glucagon. Glucagon receptors have been shown to couple to both $G\alpha_s$ and $G\alpha_q$, resulting in the elevation of cAMP or Ca^{2+} levels, respectively. Perfusing the liver with physiological concentrations of glucagon (i.e. 5–50 pM) (Emmanouel *et al.* 1978; Wewer Albrechtsen *et al.* 2016) did not induce a detectable $[Ca^{2+}]_c$ response, whereas increasing the dose a 1000-fold (5–50 nM) only generated asynchronous $[Ca^{2+}]_c$ increases in a limited number of individual hepatocytes, predominately in the periportal zone (Gaspers & Thomas, 2005). These results indicate that the picomolar concentrations of glucagon used here only activate the cAMP/PKA pathway.

The most probable mechanism of glucagon action involves the PKA-dependent phosphorylation of type1 and 2 IP_3 receptors, the major isoforms expressed in hepatocytes. PKA phosphorylation does not lead to direct opening of the channel but, instead, increases the open probability of the channel by IP_3 (Wagner *et al.* 2008; Betzenhauser *et al.* 2009). In permeabilized hepatocytes, this activation leads to a leftward shift in the dose response for IP_3-induced Ca^{2+} release (i.e. a decrease in the EC_{50}) (Bird *et al.* 1993; Hajnóczky *et al.* 1993). Thus, glucagon-induced phosphorylation of hepatic IP_3 receptors by PKA should decrease the $[IP_3]$ required to open the channel, again making the liver more excitable and therefore responsive to IP_3-linked agonists. In the presence of glucagon, the small number of individual hepatocytes (mostly in the periportal zone) that respond directly to threshold concentrations of vasopressin can act as pacemaker cells to drive Ca^{2+} waves through the rest of the lobule. In this case, the combination of glucagon and subthreshold vasopressin serves to establish the excitable lobular syncytium, and vasopressin acting on a subset of more sensitive periportal cells also acts as the initiating signal for the intercellular Ca^{2+} waves. The glucagon-dependent sensitization of IP_3 receptor Ca^{2+} channels reduces the threshold for IP_3 to elicit a Ca^{2+} signal, decreasing the time required to regenerate the propagating second messenger in each sequential hepatocyte along the hepatic plate and facilitating the recruitment of all hepatocytes in the lobule.

The data reported in the present study demonstrate the importance of the functional lobular syncytium in

setting the sensitivity of the liver to Ca^{2+}-dependent glucogenic hormones, as well as providing a means to integrate and amplify the metabolic response to multiple regulatory inputs. This is especially important at the physiologically-relevant low levels of circulating hormones to which the liver is typically exposed *in vivo*. Moreover, the propagation of Ca^{2+} waves across the lobule provides a means to amplify the response to local sympathetic neuronal output, as well as to tune this amplification to systemic endocrine status. Because the excitability of the tissue is an analogue function of the systemic hormone level, at least in the low physiological range, the extent and velocity of Ca^{2+} wave propagation, as well as the number of lobular units engaged, is expected to be determined by the concentration of the circulating hormone. The role of glucagon in establishing tissue excitability to Ca^{2+}-dependent hormones, and hence the extent of Ca^{2+} wave propagation and recruitment of hepatocytes to respond, is another novel finding that illuminates the importance of intercellular communication in the liver. The synergistic enhancement of $[Ca^{2+}]_c$ increases and intercellular Ca^{2+} waves may explain how modest increases in blood vasopressin concentrations lead to hyperglycaemia and the development of a pre-diabetic state (Nakamura *et al.* 2017; Taveau *et al.* 2017). Although, in the present study, we used vasopressin to avoid the dual signalling pathways and vascular effects mediated by catecholamines, it is expected that systemic epinephrine release from the adrenal glands will act in a similar manner. Importantly, we show that the synergistic effect of multiple stimuli to co-ordinate intralobular Ca^{2+} waves is associated with significant increases in hepatic glucose production. Thus, the lobular organization of Ca^{2+} signalling is an important determinant of endocrine regulation of liver function.

References

Assimacopoulos-Jeannet FD, Blackmore PF & Exton JH (1977). Studies on alpha-adrenergic activation of hepatic glucose output. Studies on role of calcium in alpha-adrenergic activation of phosphorylase. *J Biol Chem* **252**, 2662–2669.

Atri A, Amundson J, Clapham D & Sneyd J (1993). A single-pool model for intracellular calcium oscillations and waves in the *Xenopus laevis* oocyte. *Biophys J* **65**, 1727–1739.

Balle C, Beuers U, Engelhardt R & Jungermann K (1987). Intracellular mechanism of action of sympathetic hepatic nerves on glucose and lactate balance in perfused rat liver. *Eur J Biochem* **170**, 193–199.

Bartlett PJ, Gaspers LD, Pierobon N & Thomas AP (2014). Calcium-dependent regulation of glucose homeostasis in the liver. *Cell Calcium* **55**, 306–316.

Baylis PH & Heath DA (1977). Plasma-arginine-vasopressin response to insulin-induced hypoglycaemia. *Lancet* **2**, 428–430.

Baylis PH & Robertson GL (1980). Vasopressin response to 2-deoxy-D-glucose in the rat. *Endocrinology* **107**, 1970–1974.

Bernard C (1854). *Lecons de Physiologie experimentale.*

Berridge MJ (2016). The inositol trisphosphate/calcium signaling pathway in health and disease. *Physiol Rev* **96**, 1261–1296.

Betzenhauser MJ, Fike JL, Wagner LE, 2nd & Yule DI (2009). Protein kinase A increases type-2 inositol 1,4,5-trisphosphate receptor activity by phosphorylation of serine 937. *J Biol Chem* **284**, 25116–25125.

Beuers U, Beckh K & Jungermann K (1986). Control of ketogenesis in the perfused rat liver by the sympathetic innervation. *Eur J Biochem* **158**, 19–24.

Binet A, Berthon B & Claret M (1985). Hormone-induced increase in free cytosolic calcium and glycogen phosphorylase activation in rat hepatocytes incubated in normal and low-calcium media. *Biochem J* **228**, 565–574.

Bird GS, Burgess GM & Putney JW, Jr (1993). Sulfhydryl reagents and cAMP-dependent kinase increase the sensitivity of the inositol 1,4,5-trisphosphate receptor in hepatocytes. *J Biol Chem* **268**, 17917–17923.

Blackmore PF, Brumley FT, Marks JL & Exton JH (1978). Studies on alpha-adrenergic activation of hepatic glucose output. Relationship between alpha-adrenergic stimulation of calcium efflux and activation of phosphorylase in isolated rat liver parenchymal cells. *J Biol Chem* **253**, 4851–4858.

Bruinstroop E, Pei L, Ackermans MT, Foppen E, Borgers AJ, Kwakkel J, Alkemade A, Fliers E & Kalsbeek A (2012). Hypothalamic neuropeptide Y (NPY) controls hepatic VLDL-triglyceride secretion in rats via the sympathetic nervous system. *Diabetes* **61**, 1043–1050.

Brunner DB, Burnier M & Brunner HR (1983). Plasma vasopressin in rats: effect of sodium, angiotensin, and catecholamines. *Am J Physiol Heart Circ Physiol* **244**, H259–H265.

Buijs RM, la Fleur SE, Wortel J, Van Heyningen C, Zuiddam L, Mettenleiter TC, Kalsbeek A, Nagai K & Niijima A (2003). The suprachiasmatic nucleus balances sympathetic and parasympathetic output to peripheral organs through separate preautonomic neurons. *J Comp Neurol* **464**, 36–48.

Burgess GM, Bird GS, Obie JF & Putney JW, Jr (1991). The mechanism for synergism between phospholipase C- and adenylylcyclase-linked hormones in liver. Cyclic AMP-dependent kinase augments inositol trisphosphate-mediated Ca^{2+} mobilization without increasing the cellular levels of inositol polyphosphates. *J Biol Chem* **266**, 4772–4781.

Clair C, Tran D, Boucherie S, Claret M, Tordjmann T & Combettes L (2003). Hormone receptor gradients supporting directional Ca^{2+} signals: direct evidence in rat hepatocytes. *J Hepatol* **39**, 489–495.

Clapham DE (1995). Calcium signaling. *Cell* **80**, 259–268.

Dunn FL, Brennan TJ, Nelson AE & Robertson GL (1973). The role of blood osmolality and volume in regulating vasopressin secretion in the rat. *J Clin Invest* **52**, 3212–3219.

Emmanouel DS, Jaspan JB, Rubenstein AH, Huen AH, Fink E & Katz AI (1978). Glucagon metabolism in the rat. *J Clin Invest* **62**, 6–13.

Exton JH (1987). Mechanisms of hormonal regulation of hepatic glucose metabolism. *Diabetes-Metab Rev* **3**, 163–183.

Fyhrquist F, Tikkanen I & Linkola J (1981). Plasma vasopressin concentration and renin in the rat: effect of hydration and hemorrhage. *Acta Physiol Scand* **113**, 507–510.

Gardemann A & Jungermann K (1986). Control of glucose balance in the perfused rat liver by the parasympathetic innervation. *Biol Chem Hoppe Seyler* **367**, 559–566.

Gardemann A, Puschel GP & Jungermann K (1992). Nervous control of liver metabolism and hemodynamics. *Eur J Biochem* **207**, 399–411.

Gardemann A, Strulik H & Jungermann K (1987). Nervous control of glycogenolysis and blood flow in arterially and portally perfused liver. *Am J Physiol Endocrinol Metab* **253**, E238–E245.

Garrison JC, Borland MK, Florio VA & Twible DA (1979). The role of calcium ion as a mediator of the effects of angiotensin II, catecholamines, and vasopressin on the phosphorylation and activity of enzymes in isolated hepatocytes. *J Biol Chem* **254**, 7147–7156.

Gaspers LD, Bartlett PJ, Politi A, Burnett P, Metzger W, Johnston J, Joseph SK, Hofer T & Thomas AP (2014). Hormone-induced calcium oscillations depend on cross-coupling with inositol 1,4,5-trisphosphate oscillations. *Cell Rep* **9**, 1209–1218.

Gaspers LD, Patel S, Morgan AJ, Anderson PA & Thomas AP (2001). Monitoring generation and propagation of calcium signals in multicellular preparations. In *Calcium Signalling: A Practical Approach*, ed. Tepikin A, pp. 155–175. Oxford University Press, Oxford.

Gaspers LD & Thomas AP (2005). Calcium signaling in liver. *Cell Calcium* **38**, 329–342.

Gaspers LD & Thomas AP (2008). Calcium-dependent activation of mitochondrial metabolism in mammalian cells. *Methods* **46**, 224–232.

Grundy D (2015). Principles and standards for reporting animal experiments in The Journal of Physiology and Experimental Physiology. *J Physiol* **593**, 2547–2549.

Hajnóczky G, Gao E, Nomura T, Hoek JB & Thomas AP (1993). Multiple mechanisms by which protein kinase A potentiates inositol 1,4,5-trisphosphate-induced Ca2+ mobilization in permeabilized hepatocytes. *Biochem J* **293**, 413–422.

Hajnóczky G, Robb-Gaspers LD, Seitz MB & Thomas AP (1995). Decoding of cytosolic calcium oscillations in the mitochondria. *Cell* **82**, 415–424.

Hartmann H, Beckh K & Jungermann K (1982). Direct control of glycogen metabolism in the perfused rat liver by the sympathetic innervation. *Eur J Biochem* **123**, 521–526.

Hems DA & Whitton PD (1973). Stimulation by vasopressin of glycogen breakdown and gluconeogenesis in the perfused rat liver. *Biochem J* **136**, 705–709.

Hirata K, Pusl T, O'Neill AF, Dranoff JA & Nathanson MH (2002). The type II inositol 1,4,5-trisphosphate receptor can trigger Ca^{2+} waves in rat hepatocytes. *Gastroenterology* **122**, 1088–1100.

Jiang G & Zhang BB (2003). Glucagon and regulation of glucose metabolism. *Am J Physiol Endocrinol Metab* **284**, E671–E678.

Lechleiter J, Girard S, Peralta E & Clapham D (1991). Spiral calcium wave propagation and annihilation in *Xenopus laevis* oocytes. *Science* **252**, 123–126.

Leite MF, Hirata K, Pusl T, Burgstahler AD, Okazaki K, Ortega JM, Goes AM, Prado MA, Spray DC & Nathanson MH (2002). Molecular basis for pacemaker cells in epithelia. *J Biol Chem* **277**, 16313–16323.

McCuskey RS (2004). Anatomy of efferent hepatic nerves. *Anat Rec A Discov Mol Cell Evol Biol* **280**, 821–826.

Nakamura K, Velho G & Bouby N (2017). Vasopressin and metabolic disorders: translation from experimental models to clinical use. *J Intern Med* **282**, 298–309.

Nathanson MH, Burgstahler AD, Mennone A, Fallon MB, Gonzalez CB & Saez JC (1995). Ca^{2+} waves are organized among hepatocytes in the intact organ. *Am J Physiol Gastrointest Liver Physiol* **269**, G167–G171.

Niijima A & Fukuda A (1973). Release of glucose from perfused liver preparation in response to stimulation of the splanchnic nerves in the toad. *Jpn J Physiol* **23**, 497–508.

Ostrowski NL, Young WS, 3rd, Knepper MA & Lolait SJ (1993). Expression of vasopressin V1a and V2 receptor messenger ribonucleic acid in the liver and kidney of embryonic, developing, and adult rats. *Endocrinology* **133**, 1849–1859.

Robb-Gaspers LD & Thomas AP (1995). Coordination of Ca^{2+} signaling by intercellular propagation of Ca^{2+} waves in the intact liver. *J Biol Chem* **270**, 8102–8107.

Rooney TA, Joseph SK, Queen C & Thomas AP (1996). Cyclic GMP induces oscillatory calcium signals in rat hepatocytes. *J Biol Chem* **271**, 19817–19825.

Rooney TA, Sass EJ & Thomas AP (1989). Characterization of cytosolic calcium oscillations induced by phenylephrine and vasopressin in single fura-2-loaded hepatocytes. *J Biol Chem* **264**, 17131–17141.

Rooney TA, Sass EJ & Thomas AP (1990). Agonist-induced cytosolic calcium oscillations originate from a specific locus in single hepatocytes. *J Biol Chem* **265**, 10792–10796.

Sannemann J, Beckh K & Jungermann K (1986). Control of glycogenolysis and hemodynamics in perfused rat liver by the sympathetic innervation. Dependence on stimulation frequency and duration. *Biol Chem Hoppe Seyler* **367**, 401–409.

Scholz R, Thurman RG, Williamson JR, Chance B & Bucher T (1969). Flavin and pyridine nucleotide oxidation-reduction changes in perfused rat liver. I. Anoxia and subcellular localization of fluorescent flavoproteins. *J Biol Chem* **244**, 2317–2324.

Shimazu T (1987). Neuronal regulation of hepatic glucose metabolism in mammals. *Diabetes-Metab Rev* **3**, 185–206.

Shimazu T (1996). Innervation of the liver and glucoregulation: roles of the hypothalamus and autonomic nerves. *Nutrition* **12**, 65–66.

Shimazu T & Fukuda A (1965). Increased activities of glycogenolytic enzymes in liver after splanchnic-nerve stimulation. *Science* **150**, 1607–1608.

Shimazu T, Fukuda A & Ban T (1966). Reciprocal influences of the ventromedial and lateral hypothalamic nuclei on blood glucose level and liver glycogen content. *Nature* **210**, 1178–1179.

Shimazu T & Ogasawara S (1975). Effects of hypothalamic stimulation on gluconeogenesis and glycolysis in rat liver. *Am J Physiol* **228**, 1787–1793.

Taveau C, Chollet C, Bichet DG, Velho G, Guillon G, Corbani M, Roussel R, Bankir L, Melander O & Bouby N (2017). Acute and chronic hyperglycemic effects of vasopressin in normal rats: involvement of V1A receptors. *Am J Physiol Endocrinol Metab* **312**, E127–E135.

Taylor CW (2017). Regulation of IP_3 receptors by cyclic AMP. *Cell Calcium* **63**, 48–52.

Thevenaz P, Ruttimann UE & Unser M (1998). A pyramid approach to subpixel registration based on intensity. *IEEE Trans Image Process* **7**, 27–41.

Thomas AP, Alexander J & Williamson JR (1984). Relationship between inositol polyphosphate production and the increase of cytosolic free Ca^{2+} induced by vasopressin in isolated hepatocytes. *J Biol Chem* **259**, 5574–5584.

Ulken V, Puschel GP & Jungermann K (1991). Increase in glucose and lactate output and perfusion resistance by stimulation of hepatic nerves in isolated perfused rat liver: role of alpha 1-, alpha 2-, beta 1- and beta 2-receptors. *Biol Chem Hoppe Seyler* **372**, 401–409.

Wagner LE, 2nd, Joseph SK & Yule DI (2008). Regulation of single inositol 1,4,5-trisphosphate receptor channel activity by protein kinase A phosphorylation. *J Physiol* **586**, 3577–3596.

Wang Y, Li G, Goode J, Paz JC, Ouyang K, Screaton R, Fischer WH, Chen J, Tabas I & Montminy M (2012). Inositol-1,4,5-trisphosphate receptor regulates hepatic gluconeogenesis in fasting and diabetes. *Nature* **485**, 128–132.

Wewer Albrechtsen NJ, Kuhre RE, Windelov JA, Orgaard A, Deacon CF, Kissow H, Hartmann B & Holst JJ (2016). Dynamics of glucagon secretion in mice and rats revealed using a validated sandwich ELISA for small sample volumes. *Am J Physiol Endocrinol Metab* **311**, E302–E309.

Woods NM, Cuthbertson KS & Cobbold PH (1987). Agonist-induced oscillations in cytoplasmic free calcium concentration in single rat hepatocytes. *Cell Calcium* **8**, 79–100.

Yamamoto T, Iwai M, Kimura S & Shimazu T (1995). The mechanism of action of hepatic sympathetic nerves on ketone-body output from perfused rat liver. The effect of the interaction of noradrenaline with ATP on the release of beta-hydroxybutyrate. *Eur J Biochem* **234**, 466–471.

Yi CX, la Fleur SE, Fliers E & Kalsbeek A (2010). The role of the autonomic nervous liver innervation in the control of energy metabolism. *Biochim Biophys Acta* **1802**, 416–431.

Additional information

Competing interests

The authors declare that they have no competing interests.

Author contributions

NP and LDG performed the confocal calcium imaging studies and glucose measurements. LDG and APT designed the study. NP, LDG and APT carried out data analysis and wrote the paper. All of the authors approved the final version of the manuscript submitted for publication. All authors agree to be accountable for all aspects of the work in ensuring that questions related to the accuracy or integrity of any part of the work are appropriately investigated and resolved. All authors qualify for authorship, and all those who qualify for authorship are listed.

Funding

This work was supported, in whole or in part, by The Thomas P. Infusino Endowment and National Institutes of Health Grants DK082954 and AI099277 (to APT) and Grant AA017752 (to LDG).

Acknowledgements

We thank Dr Paula Bartlett for helpful discussions during the execution of the study and Dr Josh Berlin for help with setting up the electrical stimulation protocol.

Supporting information

Additional supporting information may be found online in the Supporting Information section at the end of the article.

Movie S1. Corresponding to Fig. 1 and showing the perfusion and washout of F-BSA in an intact perfused rat liver.

Movie S2. Corresponding to Fig. 2 and showing that perfusing the liver with 40 pM vasopressin induces intercellular $[Ca^{2+}]_c$ waves that propagate throughout the liver lobule.

Movie S3. Corresponding to Fig. 3 and showing that electrical stimulation induces localized intercellular $[Ca^{2+}]_c$ waves in the intact perfused rat liver.

Movie S4. Corresponding to Fig. 4 and showing repetitive intercellular $[Ca^{2+}]_c$ waves induced by electrical stimulation.

Movie S5. Corresponding to Fig. 6 and showing that a subthreshold dose of vasopressin induces asynchronous $[Ca^{2+}]_c$ increases throughout the hepatic lobule. The movie also shows that low-frequency (4 V, 4 Hz) and high-frequency (10 V, 10 Hz) electrical stimulation synergizes with subthreshold dose of vasopressin to produce co-ordinated intercellular $[Ca^{2+}]_c$ waves that propagate across the entire lobule.